Title: Thermally Rearranged Polymer Membranes Containing Tröger's Base Units with Exceptional Performance for Air Separations

Authors: Stephen M. Meckler; Jonathan E. Bachman; Benjamin P. Robertson; Chenhui Zhu; Jeffrey R. Long; Brett A. Helms, PhD

To be cited as: 10.1002/anie.201800556

Link to VoR: https://doi.org/10.1002/anie.201800556

Thermally Rearranged Polymer Membranes Containing Tröger's Base Units with Exceptional Performance for Air Separations

Stephen M. Meckler, Jonathan E. Bachman, Benjamin P. Robertson, Chenhui Zhu, Jeffrey R. Long, and Brett A. Helms*

Abstract: The influence of segmental chain motion on the gas separation performance of thermally rearranged (TR) polymer membranes is established for TR polybenzoxazoles featuring Tröger's base (TB) monomer subunits as exceptionally rigid sites of contortion along the polymer backbone. These polymers are accessed from solution-processable *ortho*-acetate functionalized polyimides, which are readily synthesized as high molecular-weight polymers for membrane casting. We find that thermal rearrangement leads to a small increase in *d*-spacing between polymer chains and a dramatic pore-network reconfiguration that increases both membrane permeability and O_2/N_2 selectivity, putting its performance above the 2015 upper bound.

Mass transport across polymer membranes is mediated by segmental chain motion of the polymer backbone.[1] Consequently, increased backbone rigidity improves diffusive selectivity, albeit at the expense of permeability. To enhance permeability as well as selectivity, measures to increase inter-chain spacing are often required. Within this framework of polymer design, permeability-selectivity tradeoffs manifest as upper bounds to membrane performance, as articulated by Robeson.[2,3] Upper-bound polymers for membranes, such as polymers of intrinsic microporosity (PIMs) and TR polymers, are thus highly contorted, inefficiently packed, and glassy.[4] To advance beyond these limits, new polymer backbones are needed that incorporate more rigid contortion sites that introduce free-volume elements in the membrane and slow segmental chain motion for higher diffusive selectivity, while also incorporating a means to increase inter-chain spacing—e.g., via controlled solid-state chemical rearrangements—to further enhance membrane permeability.

Here we show that rationally designed, conformationally rigid monomers, when incorporated into TR polybenzoxazole membranes, yield highly permeable, size-selective micropore networks with exceptional discrimination between gases with small diffusion correlation diameters, including dioxygen and dinitrogen. Key to the success of this approach is the implementation of TB as the site of contortion along the TR polymer backbone (Figure 1). Perturbations to the dihedral angle of TB incur substantially higher energetic penalties than spiro-centers used in conventional TR polymers;[5] as a result, solid-state decarboxylation of *ortho*-functional polyimides containing these inflexible moieties yields rigid-rod polybenzoxazole membranes[6] with small pores that enhance permeability and, for multiple important gas pairs, selectivity. This new class of TR polymers is accessed through *ortho*-acetate functionalized Tröger's base polyimide precursors: e.g., 6FDA-AcTB **1**, ODPA-AcTB **2**, and BPADA-AcTB **3** (Scheme 1). Notably, thermal rearrangement of 6FDA-AcTB **1** to 6FDA-TR-TB **4** produces membranes with a unique pore architecture that endows them with an O_2 permeability of 108 Barrer and O_2/N_2 selectivity of 8.9, placing the performance above the 2015 air-separation upper bound and highlighting new opportunities in membrane design with this strategy.[7]

Our approach provides distinct advantages over state-of-the-art membrane materials for air separations. Traditional glassy polyimides (PIs) fall below the Robeson upper bound, and systems incorporating these membranes are permeability-limited for their range of selectivities.[7,8] Solution processable microporous polymers, including PIMs[5,9] and PIM-PIs,[10] provide permeability gains over polyimides, albeit with little to no gains in selectivity; as such, their use in air separations comes with added system complexity and cost associated with low product recovery.[7] Selectivity gains over PIMs with TR polymers are thus attractive for air separations, but commensurate permeability gains are needed to fully realize the separation potential of TR polymer membranes.[8] In particular, what is lacking is a dedicated means of rigidifying the membrane while also increasing inter-chain spacing, a method uniquely implemented here.

To access conformationally rigid TR polymer membranes, we synthesized *ortho*-acetate precursor polyimides (AcTBs) that incorporate bicyclic TB units such that the thermal rearrangement yields a benzoxazole on each aromatic ring of the foundational architectural motif. AcTBs were synthesized through the condensation polymerization of *ortho*-hydroxy Tröger's base diamine **6** with a desired dianhydride (Scheme 1).

[*] S. M. Meckler, B. P. Robertson, Dr. B. A. Helms,
The Molecular Foundry
Lawrence Berkeley National Laboratory
1 Cyclotron Rd., Berkeley CA 94720
E-mail: bahelms@lbl.gov

S. M. Meckler, Prof. J. R. Long
Department of Chemistry
The University of California, Berkeley
Berkeley, CA 94720

Dr. J. E. Bachman, Prof. J. R. Long
Department of Chemical and Biomolecular Engineering
The University of California, Berkeley
Berkeley, CA 94720

C. Zhu
Advanced Light Source
Lawrence Berkeley National Laboratory
1 Cyclotron Rd., Berkeley CA 94720

Prof. J. R. Long, Dr. B. A. Helms
Materials Sciences Division
Lawrence Berkeley National Laboratory
1 Cyclotron Rd., Berkeley CA 94720

Supporting information for this article is given via a link at the end of the document.

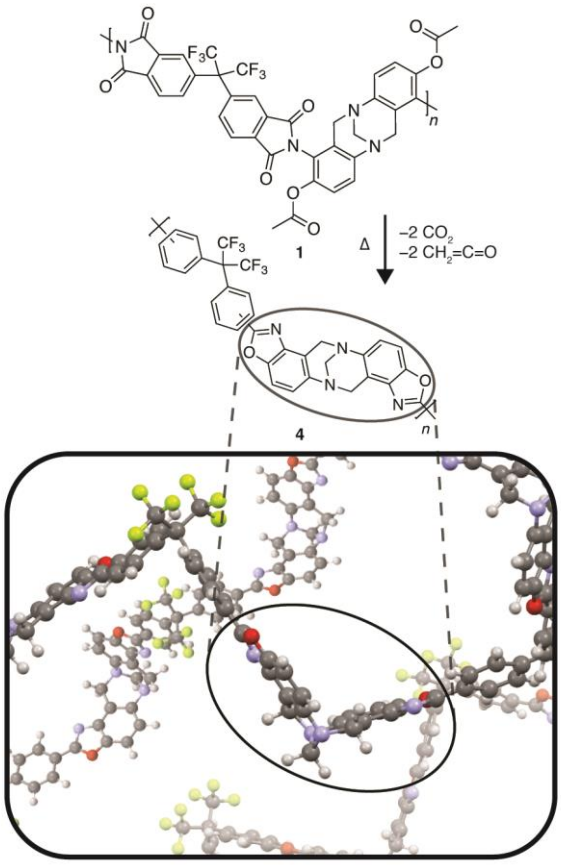

Figure 1. Thermal rearrangement reaction leading to a polybenzoxazole with Tröger's base sub-units.

The diamine monomer was synthesized through the reaction of 4-amino-2-nitrophenol **5** with paraformaldehyde followed by hydrogenation of the nitro groups. Single-crystal X-ray diffraction revealed that the amine substituents are regiospecifically *ortho* to the Tröger's base bridge, flanked on both sides by methylene and hydroxyl groups. Steric hindrance at the amine potentially limits access to high molecular weight polymers, but we overcame this limitation by silylating the amine prior to polymerization using chlorotrimethylsilane (TMS-Cl), 4-(dimethylamino)pyridine (DMAP) as a silylation catalyst, and pyridine as an acid scavenger.[11] Importantly, silylation increases electron density on the amine and lowers the activation barrier for polymerization.[12] After silylation, the dianhydride monomer was introduced into the reaction mixture to begin polymerization. Dehydration of the resulting polymer with an excess of acetic anhydride yielded the polyimide, whose *ortho*-hydroxy groups were concomitantly acetylated. The resulting AcTB polymers possessed high molecular weights (Figure S1) and excellent solubility for membrane casting.

To assess the scope of this polymerization scheme and understand architectural outcomes, AcTB polymers **1**–**3** were synthesized from three different dianhydride monomers: 4,4′-(hexafluoroisopropylidene)diphthalic anhydride (6FDA), 4,4′-oxydiphthalic anhydride (ODPA), and 4,4′-(4,4′-isopropylidenediphenoxy)*bis*(phthalic anhydride) (BPADA). No glass transition was observed up to 325 °C for 6FDA-AcTB **1** or ODPA-AcTB **2**, but a clear transition was recorded at T_g = 294 °C for BPADA-AcTB **3** (Figure S2). The BET surface area, as measured by nitrogen gas adsorption at 77 K, dropped precipitously with the removal of bulky trifluoromethyl substituents (172 m^2 g^{-1} for 6FDA-AcTB **1** *vs.* 51 m^2 g^{-1} for ODPA-AcTB **2**, Figure S3), and when excess flexibility was introduced in BPADA-AcTB, no N_2 uptake was observed. These results demonstrate that the physical properties and pore networks of AcTB polymers (and films) are tunable through chemical design of the dianhydride. Further, the highly glassy and porous nature of 6FDA-AcTB **1** suggests it would be the most promising membrane material for air separations; as such, it was further investigated through the full TR reaction pathway.

TR-TB polymer membranes accessed through the solid-state decarboxylation of AcTB polyimide films feature the rigidity of the polybenzoxazole structure, enhanced porosity from polymer chain reconfiguration, and complementary intra-chain rigidity and frustrated inter-chain packing from the TB sub-unit. To understand the thermal reaction pathway through which 6FDA-AcTB **1** proceeds, we employed thermo-gravimetric analysis coupled with mass-spectrometry (TGA-MS). During thermal rearrangement, two mass loss events are expected: the first loss results from elimination of acetate groups, producing ketene and leaving behind a hydroxyl group;[13] carbon dioxide is then driven off during rearrangement to the benzoxazole. Figure 2a shows total mass loss and relative intensities of the ketene and carbon dioxide mass peaks as a function of temperature. Acetate loss begins around 300 °C and peaks just below 400 °C. As the thermal rearrangement reactions can be sequential, 400 °C is considered the lower-bound temperature for thermal rearrangement in this system. Carbon dioxide evolution is marked by a local maximum around 450 °C, coinciding with a peak in the first derivative mass loss (Figure S4a), consistent with the proposed polybenzoxazole formation mechanism.

To maximize conversion to the benzoxazole while minimizing polymer backbone decomposition, care must be taken in developing thermal rearrangement protocols, which typically involve a high-temperature isothermal soak. Ideally, the experimental mass loss is equivalent to the theoretical value. Isothermal TGA experiments were used to monitor TR conversion at different soak temperatures. Films were heated at 5 °C min^{-1} to 300 °C under flowing argon and held at that temperature for 1 h to fully imidize the polymer and drive off any residual solvent. The films were then heated at 5 °C min^{-1} to a final soak temperature varying between 400–440 °C. The theoretical 22.2% mass loss for complete thermal rearrangement was reached in ~7 min at 440 °C, ~27 min at 420 °C, and ~94 min at 400 °C (Figure S4b). Based on these findings, we adopted a final soak temperature of 420 °C for 30 min. Large-format membranes were thermally treated in a tube furnace under flowing argon. Thermally-treated films were insoluble in all solvents tested, as is common for TR polymers.[6]

To understand the influence of thermal treatment on analyte transport through AcTB polymer films, we measured the permeability of CO_2, O_2, N_2, and CH_4 through films of 6FDA-AcTB **1** and 6FDA-TR-TB **4**. For all four gases, permeability increases with thermal rearrangement, from 17 to 108 Barrer for O_2, 72 to 158 Barrer for CO_2, 3.9 to 12 Barrer for N_2, and 3.3 to

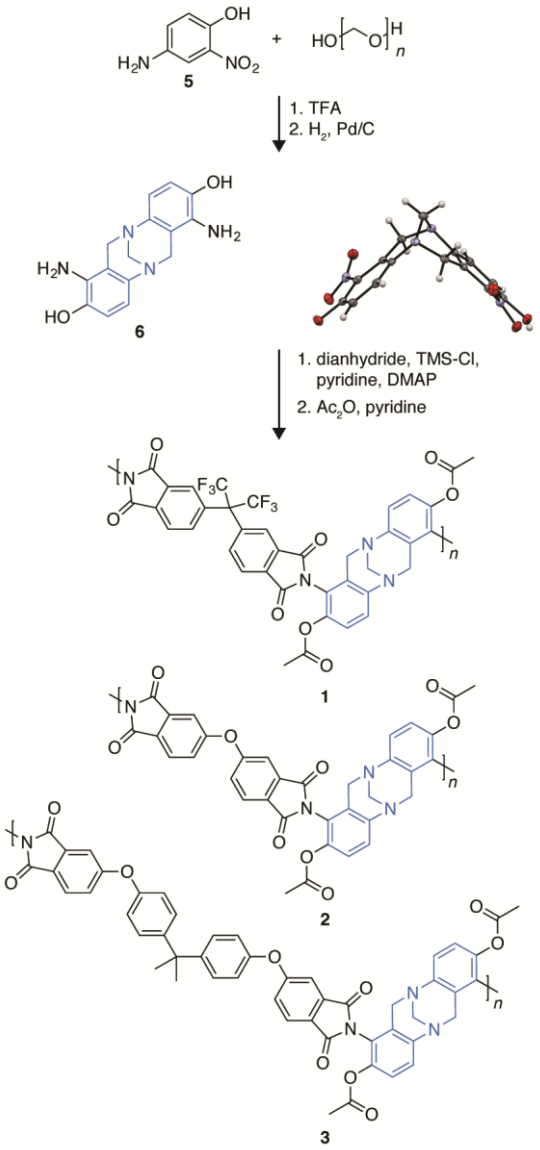

Scheme 1. Synthesis of *ortho*-acetate polyimides 6FDA-AcTB **1**, ODPA-AcTB **2**, and BPADA-AcTB **3**. The single-crystal XRD structure of the dinitro precursor to diamine **6** demonstrates the contortion of the Tröger's base unit.

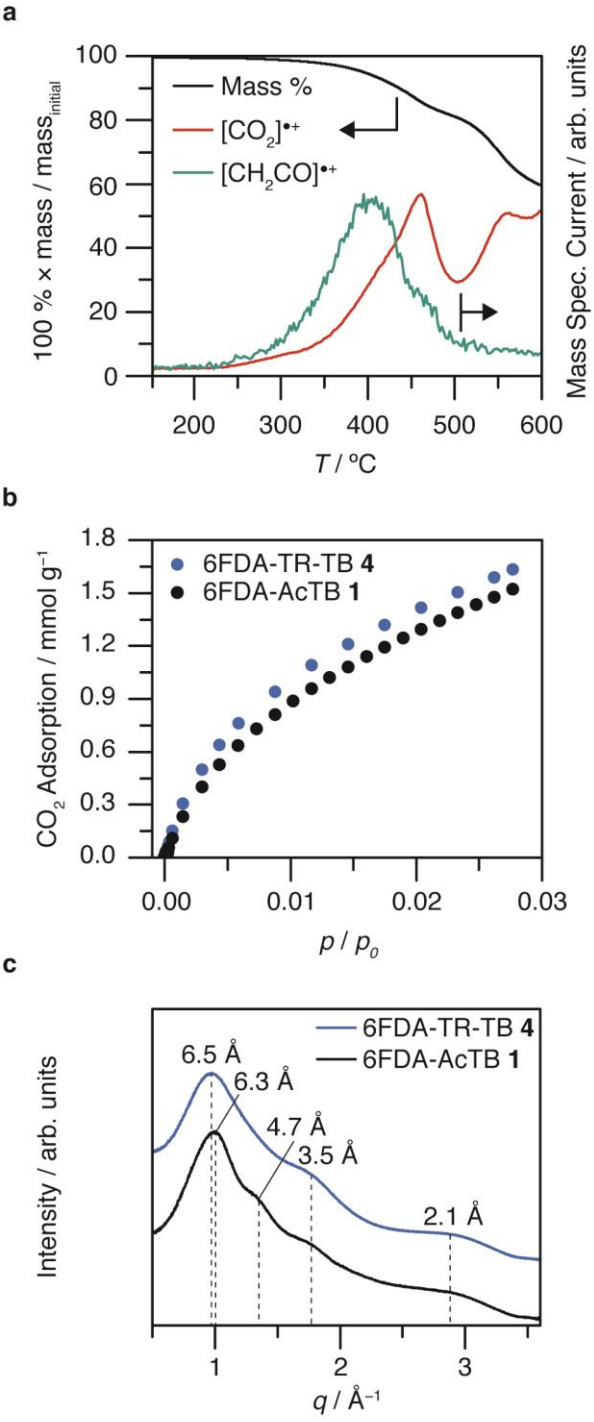

Figure 2. Characterization of the thermal rearrangement reaction and the related structural evolution. a) TGA-MS of 6FDA-AcTB **1** heated to 600 °C at a ramp rate of 10 °C min^{-1}. b) CO_2 adsorption isotherms at 273 K and c) WAXS patterns of 6FDA-AcTB **1** and 6FDA-TR-TB **4**.

6.7 Barrer for CH_4. Smaller gases generally exhibit the greatest enhancements (Figure 3a). The less pronounced increase in CO_2 permeability, which is largely dictated by solubility, suggests that the observed enhancements are diffusivity driven. The increase in O_2 permeability is most significant, improving both permeability and selectivity for O_2/N_2 separations and placing the membrane far above the 2008 upper bound[3] and slightly above the more recently suggested 2015 upper bound (Figure 3b).[7]

The chemical origins of these membrane performance enhancements were investigated spectroscopically. Carbon X-ray photoelectron spectroscopy (XPS) revealed that both 6FDA-AcTB **1** and 6FDA-TR-TB **4** have a broad peak near 284 eV, as well as a small peak at 293 eV from trifluoromethyl carbons (Figure S5a). Of note, the carbonyl carbon peak near 288 eV in the 6FDA-AcTB **1** spectrum is greatly diminished in the 6FDA-TR-TB **4** spectrum. This result suggests successful evolution of the acetate groups and reaction of the imide sites, as is

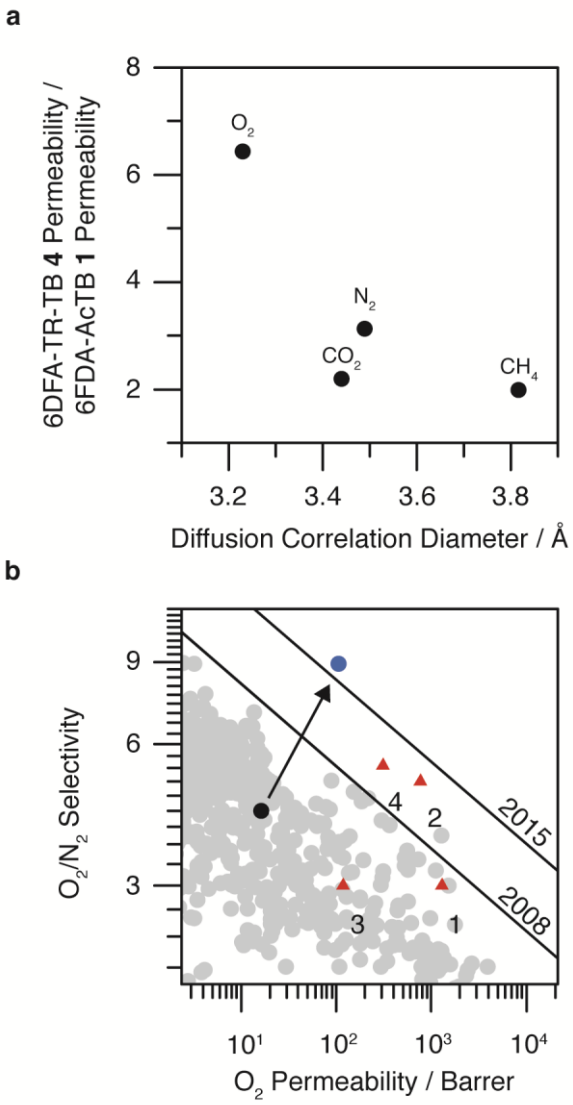

Figure 3. a) Permeability enhancements *vs.* gas diffusion correlation diameter[14] from the thermal rearrangement of 6FDA-AcTB **1** to 6FDA-TR-TB **4**. b) 6FDA-AcTB **1** (black) and 6FDA-TR-TB **4** (blue) membrane performance at 1.9 atm and 35 °C plotted against the upper bound for air separations. Red triangles mark the performance of previously reported TR polymers: 1 – cTR-450,[15] 2 – tTR-450, 3 – spiroTR-PBO-6F,[16] and 4 – TR TDA1-APAF.[17] Grey circles represent polymer membranes reported in the literature.

expected during benzoxazole formation. Because overlapping signals in the large XPS features near 284 eV were difficult to deconvolute into meaningful components, FT-IR spectroscopy was used to further investigate the chemical evolution during thermal rearrangement (Figure S5b). The 6FDA-AcTB **1** spectrum contains peaks at 1774 cm^{-1} (carbonyl), 1730 cm^{-1} (carbonyl), and 1374 cm^{-1} (imide C–N) that are greatly diminished in the 6FDA-TR-TB **4** spectrum, consistent with the loss of carbonyl signal in the XPS. Furthermore, peaks at 1497 cm^{-1} and 1097 cm^{-1}, attributed to benzoxazole formation,[13] are evident in the 6FDA-TR-TB **4** spectrum. Together, this spectroscopic information supports near complete thermal rearrangement.

While restricted intra-chain mobility arising from local chemical changes can account for some membrane performance attributes, global pore-network evolution during thermal rearrangement is also important in dictating transport outcomes. Carbon dioxide adsorption isotherms collected at 273 K show higher uptake in 6FDA-TR-TB **4** *vs.* 6FDA-AcTB **1**, consistent with the predicted porosity increase and the observed permeability increase with thermal rearrangement (Figure 2b). Nonlocal DFT pore-size distributions produced from these isotherms reveal significant ultramicroporosity (i.e., pores of diameter < 7 Å, Figure S6). The isotherms and pore-size distributions were similar for both polymers, motivating further study of the pore networks with synchrotron wide-angle X-ray scattering (WAXS, Figure 2c). A small decrease in the peak position of the main scattering feature near 1 $Å^{-1}$ reflects an increase in average inter-chain *d*-spacing from 6.3 Å in 6FDA-AcTB **1** to 6.5 Å in 6FDA-TR-TB **4**. This increased inter-chain spacing is consistent with increased porosity and permeability. Notably, a shoulder feature in the 6FDA-AcTB **1** scattering pattern corresponding to 4.7 Å disappears from the 6FDA-TR-TB **4** scattering pattern, and the feature corresponding to 3.5 Å grows in relative intensity and broadness after thermal rearrangement.

These changes to the WAXS patterns with thermal rearrangement could signal the coalescence of pores into more uniform free-volume elements with spacing between the diameters of O_2 and N_2. Polymer segments too inflexible to exhibit segmental chain motion-dictated transport may be exhibiting a molecular sieving effect; such a shift in transport mechanism would explain the marked increase in O_2/N_2 selectivity despite more modest performance increases in CO_2/CH_4 and CO_2/N_2 separations (Figure S7). High-*q* scattering features in porous polymer WAXS patterns, however, sometimes reflect distances between given repeat units rather than the space between chains.[18] If the former is true, the results still signal a shift to a more uniform distribution of occupied volume in the porous material. Overall, characterization of the TR polymer pore network suggests that an increase in pore size and total porosity is responsible for the enhanced permeability while the formation of immobile size-discriminating windows enhances size-selectivity for air separations.

The exceptional performance of 6FDA-TR-TB **4** membranes and the characterization of their pore network validates our design strategy of incorporating conformationally rigid units such as TB into a TR polybenzoxazole to produce highly selective membranes without sacrificing permeability. We propose that these membranes could be relevant in applications where inert gas production is needed in confined areas, such as backfilling fuel tanks on aircraft. We note that the permselectivity of TR-TB membranes could be further tuned through the chemical structure of the dianhydride residue, but the rational design of more conformationally rigid motifs is necessary to substantially advance TR polymer membranes. Strategies to this end will likely include the development of sterically-hindered polycyclic monomers, an approach that has seen recent success in advanced PIMs.[19] Leading-Edge materials genomics screens

may be an effective tool in accelerating this discovery process.[20] The TR-TB platform reported here is an important first step and effective guidepost along this design trajectory.

Acknowledgements

This work was supported by the Center for Gas Separations Relevant to Clean Energy Technologies, an Energy Frontier Research Center funded by the U.S. Department of Energy, Office of Science, Basic Energy Sciences under Award # DE-SC0001015. BPR was supported by the U.S. Department of Energy, Office of Science, Office of Workforce Development for Teachers and Scientists (WDTS) under the Science Undergraduate Laboratory Internship (SULI) program. Portions of this work, including synthesis, characterization, and film processing, were carried out as a User Project at the Molecular Foundry, which is supported by the Office of Science, Office of Basic Energy Sciences, of the U.S. Department of Energy under Contract No. DE-AC02-05CH11231. WAXS was carried out at beamline 7.3.3 of the Advanced Light Source, which is supported by the Director, Office of Science, Office of Basic Energy Sciences, of the U.S. Department of Energy under the same contract. We thank L. Klivansky for assistance with XPS and N. Settineri for assistance with single-crystal X-ray diffraction.

Keywords: polymers • Tröger's base • gas separations • membranes • selective transport

[1] B. D. Freeman, *Macromolecules* **1999**, *32*, 375.
[2] L. M. Robeson, *J. Membr. Sci.* **1991**, *62*, 165.
[3] L. M. Robeson, *J. Membr. Sci.* **2008**, *320*, 390.
[4] a) L. M. Robeson, M. E. Dose, B. D. Freeman, D. R. Paul, *J. Membr. Sci.* **2017**, *525*, 18; b) C. Li, S. M. Meckler, Z. P. Smith, J. E. Bachman, L. Maserati, J. R. Long, B. A. Helms, *Adv. Mater.* **2018**, DOI: 10.1002/adma.201704953.
[5] M. Carta, R. Malpass-Evans, M. Croad, Y. Rogan, J. C. Jansen, P. Bernardo, F. Bazzarelli, N. B. McKeown, *Science* **2013**, *339*, 303.
[6] H. B. Park, C. H. Jung, Y. M. Lee, A. J. Hill, S. J. Pas, S. T. Mudie, E. Van Wagner, B. D. Freeman, D. J. Cookson, *Science* **2007**, *318*, 254.
[7] R. Swaidan, B. Ghanem, I. Pinnau, *ACS Macro Lett.* **2015**, *4*, 947.
[8] D. F. Sanders, Z. P. Smith, R. Guo, L. M. Robeson, J. E. McGrath, D. R. Paul, B. D. Freeman, *Polymer* **2013**, *54*, 4729.
[9] a) P. M. Budd, B. S. Ghanem, S. Makhseed, N. B. McKeown, K. J. Msayib, C. E. Tattershall, *Chem. Commun.* **2004**, *0*, 230; b) B. S. Ghanem, R. Swaidan, X. Ma, E. Litwiller, I. Pinnau, *Adv. Mater.* **2014**, *26*, 6696.
[10] a) B. S. Ghanem, N. B. McKeown, P. M. Budd, J. D. Selbie, D. Fritsch, *Adv. Mater.* **2008**, *20*, 2766; b) M. Lee, C. G. Bezzu, M. Carta, P. Bernardo, G. Clarizia, J. C. Jansen, N. B. McKeown, *Macromolecules* **2016**, *49*, 4147; c) X. Ma, M. Abdulhamid, X. Miao, I. Pinnau, *Macromolecules* **2017**, *50*, 9569.
[11] D. M. Muñoz, M. Calle, J. G. de la Campa, J. de Abajo, A. E. Lozano, *Macromolecules* **2009**, *42*, 5892.
[12] A. E. Lozano, J. de Abajo, J. G. De la Campa, *Macromol. Theory and Simul.* **1998**, *7*, 41.
[13] Z. P. Smith, D. F. Sanders, C. P. Ribeiro, R. Guo, B. D. Freeman, D. R. Paul, J. E. McGrath, S. Swinnea, *J. Membr. Sci.* **2012**, *415-416*, 558.
[14] L. M. Robeson, Z. P. Smith, B. D. Freeman, D. R. Paul, *J Membr. Sci.* **2014**, *453*, 71.
[15] S. Kim, H. J. Jo, Y. M. Lee, *J. Membr. Sci.* **2013**, *441*, 1.
[16] S. Li, H. J. Jo, S. H. Han, C. H. Park, S. Kim, P. M. Budd, Y. M. Lee, *J. Membr. Sci.* **2013**, *434*, 137.
[17] F. Alghunaimi, B. Ghanem, Y. Wang, O. Salinas, N. Alaslai, I. Pinnau, *Polymer* **2017**, *121*, 9.
[18] A. G. McDermott, G. S. Larsen, P. M. Budd, C. M. Colina, J. Runt, *Macromolecules* **2011**, *44*, 14.
[19] I. Rose, C. G. Bezzu, M. Carta, B. Comesaña-Gándara, E. Lasseuguette, M. C. Ferrari, P. Bernardo, G. Clarizia, A. Fuoco, J. C. Jansen, K. E. Hart, T. P. Liyana-Arachchi, C. M. Colina, N. B. McKeown, *Nat. Mater.* **2017**, *16*, 932.
[20] a) A. L. Ward, S. E. Doris, L. Li, M. A. Hughes, X. Qu, K. A. Persson, B. A. Helms, *ACS Cent. Sci.* **2017**, *3*, 399; b) L. C. H. Gerber, P. D. Frischmann, F. Y. Fan, S. E. Doris, X. Qu, A. M. Scheuermann, K. Persson, Y.-M. Chiang, B. A. Helms, *Nano Lett.* **2016**, *16*, 549; c) P. D. Frischmann, L. C. H. Gerber, S. E. Doris, E. Y. Tsai, F. Y. Fan, X. Qu, A. Jain, K. A. Persson, Y.-M. Chiang, B. A. Helms, *Chem. Mater.* **2015**, *27*, 6765.

COMMUNICATION

All About That Base: A thermally rearranged polybenzoxazole membrane incorporating a rigid Tröger's base site of contortion is reported. Porosimetry and X-ray scattering reveal an evolution in the membrane micropore network with thermal rearrangement that leads to state-of-the-art performance for air separations.

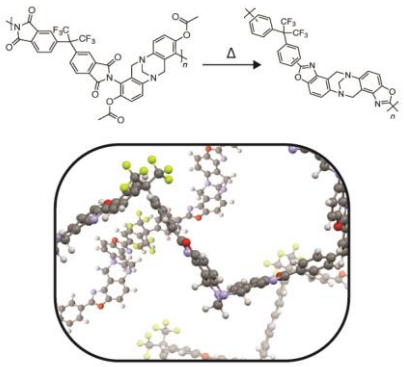

*Stephen M. Meckler, Jonathan E. Bachman, Benjamin P. Robertson, Chenhui Zhu, Jeffrey R. Long, and Brett A. Helms**

Page No. – Page No.

Thermally Rearranged Polymer Membranes Containing Tröger's Base Units with Exceptional Performance for Air Separations